Molecular Plant Pathology

MOLECULAR PLANT PATHOLOGY (2017) 18(2), 298–307 DOI: 10.1111/mpp.12392

Technical advance

Optimization of the HyPer sensor for robust real-time detection of hydrogen peroxide in the rice blast fungus

KUN HUANG[1,2], JEFF CAPLAN[1], JAMES A. SWEIGARD[3], KIRK J. CZYMMEK[4] AND NICOLE M. DONOFRIO[2,*]

[1]*BioImaging Center, Delaware Biotechnology Institute, Newark, DE 19716, USA*
[2]*Department of Plant and Soil Sciences, University of Delaware, Newark, DE 19716, USA*
[3]*DuPont Stine Haskell Research Center, 1090 Elkton Rd, Newark, DE 19711, USA*
[4]*Zeiss, 1 Zeiss Dr., Thornwood, NY 10594, USA*

SUMMARY

Reactive oxygen species (ROS) production and breakdown have been studied in detail in plant-pathogenic fungi, including the rice blast fungus, *Magnaporthe oryzae*; however, the examination of the dynamic process of ROS production in real time has proven to be challenging. We resynthesized an existing ROS sensor, called HyPer, to exhibit optimized codon bias for fungi, specifically *Neurospora crassa*, and used a combination of microscopy and plate reader assays to determine whether this construct could detect changes in fungal ROS during the plant infection process. Using confocal microscopy, we were able to visualize fluctuating ROS levels during the formation of an appressorium on an artificial hydrophobic surface, as well as during infection on host leaves. Using the plate reader, we were able to ascertain measurements of hydrogen peroxide (H_2O_2) levels in conidia as detected by the MoHyPer sensor. Overall, by the optimization of codon usage for *N. crassa* and related fungal genomes, the MoHyPer sensor can be used as a robust, dynamic and powerful tool to both monitor and quantify H_2O_2 dynamics in real time during important stages of the plant infection process.

Keywords: appressorium, codon bias, confocal imaging, HyPer sensor, *Magnaporthe oryzae*, reactive oxygen species, rice blast fungus.

INTRODUCTION

Abundant research continues to demonstrate the importance of reactive oxygen species (ROS) in a wide variety of biological processes (Lang *et al.*, 2013; Panieri *et al.*, 2013; Sun *et al.*, 2013). In animals, ROS are involved in the inflammatory response and, through their electrophilic capability, ROS contribute to the development of many serious diseases (Bystrom *et al.*, 2013; Rogers, 2002). In plants, ROS play a crucial role in growth and development, and pathogen defence (Foreman *et al.*, 2003; Kawano, 2003). For example, there are at least 152 genes involved in ROS secretion, function and signalling in *Arabidopsis thaliana* (Mittler *et al.*, 2004). During plant–pathogen interactions, ROS function in the formation of physical defence components (such as cell wall appositions) (Collinge, 2009),and in the activation of the *R* gene-mediated hypersensitive response (Delledonne *et al.*, 2001). In fungi, including the rice blast fungus that we focus on in this study, ROS have been found to play a critical role in the development of the appressorium, a key structure in pathogenesis (Brown *et al.*, 2008; Egan *et al.*, 2007; Heller and Tudzynski, 2011).

The rice blast fungus, *Magnaporthe oryzae*, causes serious disease in rice-growing countries, such as China, Korea, Japan, Vietnam and the USA (Dean *et al.*, 2005), where, recently, 5.7 million hectares of rice were destroyed (Wilson and Talbot, 2009). Because of its global importance to food production, research has focused on how this fungus initially gains entrance to the host. Infection proceeds via a dome-shaped appressorium that develops from germinated asexual conidia on the surface of a leaf. The appressorium develops via a controlled process of autophagic cell death of the conidium, followed by enormous turgor pressure forcing the appressorium to swell and penetrate the plant leaf surface via a penetration peg (Parker *et al.*, 2008). Importantly, appressoria cannot form without the production of ROS. Deletion of the ROS-generating NADPH oxidases prevents appressorial development (Egan *et al.*, 2007). It has been determined that ROS also contribute to fungal cell wall integrity, without which the pathogen cannot gain access (Skamnioti *et al.*, 2007).

The contribution of ROS in plant–fungal interactions has been closely studied in numerous additional fungal interactions spanning from pathogenic to beneficial. ROS production is essential for full virulence of the necrotrophs *Botrytis cinerea* and *Alternaria alternata* (Yang and Chung, 2012). Recently, it has also been determined that ROS are required to maintain balanced biotrophy between the fungal biotroph *Claviceps purpurea* and rye, where fungal ROS production appears to control a developmental switch

* *Correspondence*: Email: ndonof@udel.edu

in the fungus into more of a dormant, overwintering state (Schurmann *et al.*, 2013). These studies represent numerous experiments that have used genetic analysis as a tool for the dissection of the role of ROS during plant–fungal interactions; however, additional and accessible resources to study ROS dynamics during these interactions on a subcellular level have proven to be more challenging.

Nonetheless, a number of methods exist for the detection of ROS. There are at least 61 commercial products for the detection and tracking of ROS (Invitrogen™, Carlsbad, CA, USA, online resources). The dyes H_2DCFDA (2′,7′-dichlorodihydrofluorescein diacetate), Amplex Red and DAB (3,3′-diaminobenzidine) are used for hydrogen peroxide (H_2O_2) detection. DAB and H_2DCFDA are the two most widely used detection methods for H_2O_2, and are popular for the detection of this species during plant–pathogen interactions (Huang *et al.*, 2011; Yang *et al.*, 2009). Many ROS are very active with a short lifetime (10^{-5}–10^{-9} s); H_2O_2 is the only form of ROS that has a longer half-life (Cruz de Carvalho, 2008); hence, the plethora of tools for its detection. DAB is very specific to H_2O_2, but the reaction is slow (8 h) (ThordalChristensen *et al.*, 1997). In order to detect H_2O_2 generated during plant–pathogen interactions, the whole leaf or infected portion needs to be immersed in a DAB solution for approximately 8–12 h (Thordal-Christensen *et al.*, 1997), and it is usually difficult to quantify. H_2DCFDA is a membrane-permeable dye which has recently been used widely to study H_2O_2 (Huang *et al.*, 2011; Tarpey *et al.*, 2004). This dye is highly sensitive to H_2O_2, and can be utilized with confocal microscopy to obtain information about ROS at the cellular level. However, this dye is dependent on esterases. The esterase concentration can affect the results (Brubacher and Bols, 2001). Another concern with the use of H_2DCFDA is that intracellular oxidation of H_2DCF tends to be accompanied by leakage of the fluorescent product when the reaction is slow (Tarpey *et al.*, 2004), which results in improperly detected H_2O_2 levels when using this method.

In recent years, researchers have sought to rectify the issues surrounding ROS-specific dyes to quantify ROS levels, including fluorescent sensors genetically integrated into the host genome (Samalova *et al.*, 2013). HyPer, developed by Belousov *et al.* (2006), is a genetically encoded fluorescent sensor capable of detecting intracellular H_2O_2. This probe contains the circularly permuted yellow fluorescent protein (cpYFP) inserted into OxyR. OxyR is a transcription factor from *Escherichia coli* that senses H_2O_2. On activation, OxyR forms an intramolecular disulfide bond, which leads to a dramatic conformational change in the regulatory domain (Choi *et al.*, 2001). The excitation spectrum has two maxima at 420 and 500 nm, and the emission spectrum has one peak at 516 nm. HyPer is a ratiometric sensor based on the proportional decrease in its excitation peak at 420 nm to the increase in the peak at 500 nm in the presence of H_2O_2 (Belousov *et al.*, 2006). As a result, HyPer can be widely used as a quantitative and real-time measurement technique for H_2O_2 (mechanism shown in Fig. 1). Studies have also found that HyPer does not cause artefactual H_2O_2 generation (Belousov *et al.*, 2006). Several genetically encoded sensors have recently been used in plant-pathogenic fungi to explore ROS responses during exposure to plant compounds, as well as between fungal mutants. Two studies used two different sensors to examine homologues of the redox-sensitive transcription factor AP1. Heller *et al.* (2012) used roGFP, which is a reduction–oxidation-sensitive form of the green fluorescent protein (GFP), coupled to a subunit of glutaredoxin (GRx), to examine reduced glutathione (GSH) changes in the necrotrophic plant pathogen *Botrytis cinerea*, comparing GSH dynamics in wild-type versus the *BAP1* mutant. Ronen *et al.* (2013) used the HyPer construct to examine H_2O_2 levels in the necrotrophic corn pathogen *Cochliobolus heterostrophus* after exposure to plant phenolics, and a comparison was made between the wild-type and a fungal line mutant in the AP1 homologue, *CHAP1*. Both endogenous sensors demonstrated that, on exposure to ROS, the mutants took longer to recover redox homeostasis. An additional development with roGFP by Samalova *et al.* (2013) examined subtle changes in cellular status during development and infection in *M. oryzae*. The authors found that fungal pools of the antioxidant GSH remained reduced regardless of whether the fungus was infecting a resistant or susceptible host. The power of the imaging

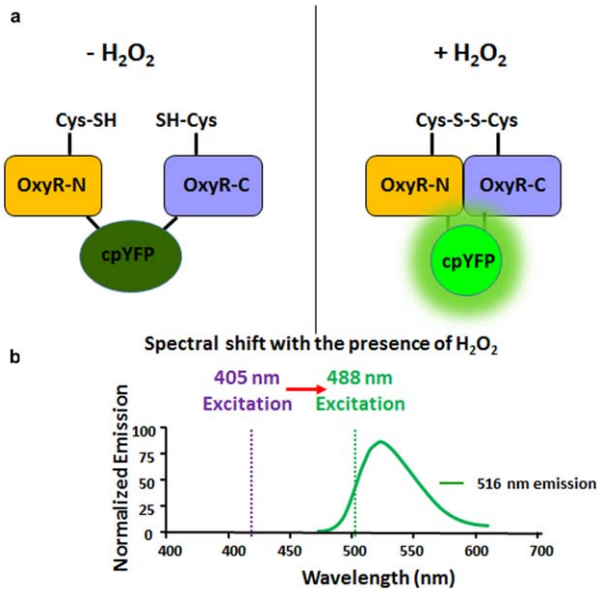

Fig. 1 Mechanism of detection of H_2O_2 with MoHyPer. (a) Domain structure of MoHyPer. In the presence of H_2O_2, a disulfide bond is formed between two cysteine (Cys) residues located in the amino (N) and carboxyl (C) domains of HyPer. The conformational change drives a ratiometric fluorescence change in circularly permuted yellow fluorescent protein (cpYFP). (b) Spectral shift from 420 nm excitation to 500 nm excitation with the presence of H_2O_2. Diagram modified from http://genomics.unl.edu/RBC_EDU/hp.html.

and quantification of the redox status in living cells has revealed these new observations in plant-pathogenic fungi.

Our study utilizes the HyPer sensor to examine ROS levels during susceptible interactions with host plants. However, it was a challenge to apply this sensor to *M. oryzae*. Our initial studies showed that transformed fungal lines either showed no fluorescence or unstable fluorescence. When comparing the codon usage preference between *M. oryzae* and HyPer, we found that HyPer and *M. oryzae* were dramatically different. We therefore designed the protein according to *Neurospora crassa* codon bias, a fungus closely related to *M. oryzae* (Dawe *et al.*, 2003). The new MoHyPer protein can be used to detect ROS concentration changes during conidial development, germination, appressorium formation and infection stages of *M. oryzae*. Importantly, we found that H_2O_2 levels in transformed lines can be easily measured using a fluorescent plate reader.

RESULTS

Codon modification and generation of MoHyPer

We sought to stably transform *M. oryzae* strain 4091-5-8, which is a pathogen of barley and easily manipulated in the laboratory (Valent *et al.*, 1991). Although we were able to identify fungal transformants that positively contained the HyPer construct via polymerase chain reaction (PCR) (data not shown), we were unable to obtain stable expression from them, and they did not yield usable results. In order to determine why the gene was not expressed, we compared the codon choices for each amino acid of the original HyPer sensor and *M. oryzae* highly expressed genes, and noticed dramatic differences in terms of codon usage. In the HyPer sensor, some rare *M. oryzae* codons were used frequently and some highly used *M. oryzae* codons were not used at all. For example, in *M. oryzae*, GGC, CTC and CCC were the most commonly used codons for glycine (46%), leucine (30%) and proline (32%), respectively. However, these codons were not common in the HyPer sequence (0%; Table S2, bold text, see Supporting Information). Indeed, codon usage in the HyPer sequence was rarely used in *M. oryzae* amino acid sequences. For example, GGA, CTA and AGG were highly used for glycine, leucine and arginine in HyPer (46%, 22% and 63%, respectively), and rarely used in *M. oryzae* (at 18%, 6% and 18%, respectively) (Table S2, red text). As a result, we modified the codons of HyPer using the DuPont Codon Optimizer site. We used the *N. crassa* codon table, as this fungus is closely related to *M. oryzae*. We then eliminated rare codons based on our comparisons in Table S2. Next, 16 pairs of primers, with 70-bp homologous sequences for each adjacent primer pair, were used to generate a new MoHyPer sequence (Table S1, see Supporting Information). The final product (1437 bp) was cloned into a fungal overexpression vector driven by the Rp27 promoter [Fig. S1, see Supporting Information; derived from the *M. oryzae* ribosomal protein 27 gene, carried by plasmid pSM565 (Bourett *et al.*, 2002)].

MoHyPer is a robust sensor and is able to detect *M. oryzae* ROS change over a broad range

First, we determined whether the MoHyPer construct in the *M. oryzae* strain containing MoHyPer protein (HyPer 9-2) was able to respond to H_2O_2. We performed H_2O_2 treatments on *M. oryzae* conidial (asexual spore) suspensions by dropping 10 μL at 5×10^4 condia/mL concentration onto glass slides and imaging the initial response using confocal microscopy. Two millimolar H_2O_2 was then added to conidial suspensions of both HyPer 9-2 and the wild-type control 4091-5-8. As shown in Fig. 2, the HyPer 9-2 strain immediately showed bright fluorescence on application of H_2O_2 in the green channel (488/516 nm) and an increase in the ratio value, which is a ratiometric representation of the H_2O_2 level. In contrast, the wild-type strain 4091-5-8 showed almost no increase in fluorescence. Neither strain showed a detectable value in the ratio channel when H_2O_2 was not present (Fig. 2). For all following images, unless otherwise indicated, the blue and green panels show images in which the samples were excited with the 405-nm wavelength laser and 488-nm wavelength laser, respectively. The intensity of the green channel was then divided by the intensity of the blue channel, and the resulting ratio indicated the H_2O_2 level, as detected by MoHyPer. We next tested whether MoHyPer was able to detect ROS level changes in *M. oryzae*. We applied exogenous H_2O_2 to conidia from the HyPer 9-2 and 4091-5-8 (wild-type) strains that had adhered to eight-well imaging chambers. The attachment and initial germination event revealed a high initial 'start' level of H_2O_2. Ten millimolar dithiothreitol (DTT) was used to reduce the background fluorescence, through its action as a known antioxidative agent. Then, 5, 10, 50, 100 and 300 μM H_2O_2 were introduced to each well, followed by a sterile water washout in between each treatment. MoHyPer was able to detect very low concentrations of H_2O_2 (Fig. 3a, ratio channel). At 100 μM, MoHyPer exhibited a higher ratio value compared with the starting level of 5 μM H_2O_2. The accompanying dose–response curve of MoHyPer showed a linear increase on increasing concentration of H_2O_2 (Fig. 3b). To rigorously test the sensitivity of the sensor, we performed a similar washout experiment with increasingly higher H_2O_2 concentrations. Even after a 40 mM H_2O_2 treatment, the water washout was able to return the sensor levels to baseline (Fig. 3c-d), confirming that our sensor is both sensitive and robust for the detection of both large and small changes in H_2O_2.

MoHyPer detects development-related changes in H_2O_2 in *M. oryzae*

After establishing that our modified MoHyPer sensor could detect H_2O_2 changes in conidia, we determined whether we could detect changing levels of H_2O_2 during spore germination and

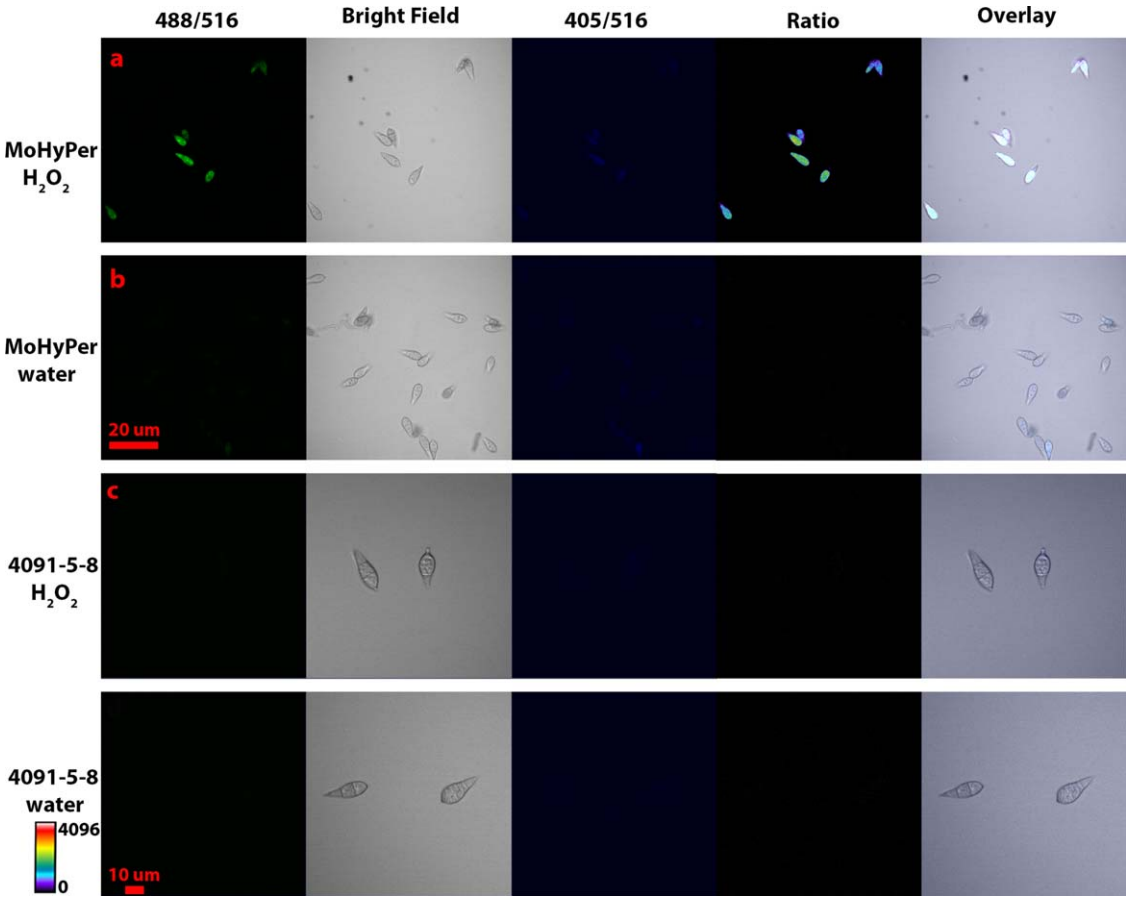

Fig. 2 MoHyPer protein senses H_2O_2. Ratio panel indicates that the signal intensity at 500 nm is increased. (a) 2 mM H_2O_2 was applied. (b) 0 mM H_2O_2 was applied. Scale bar = 20 μm for (a) and (b). (c) 2 mM H_2O_2 was applied to 4091-5-8. (d) 0 mM H_2O_2 was applied to 4091-5-8. As indicated by the scale bar, warmer colours indicate increased levels of H_2O_2. Scale bar = 10 μm for (c) and (d).

appressorial development. According to Egan *et al.* (2007), *M. oryzae* generates ROS during pre-infection-related processes, including the formation of the germ tube and development of the appressorium, the specialized infection structure. To determine whether MoHyPer is able to detect H_2O_2 during the pre-infection stage, we first investigated the production of H_2O_2 during conidial germination on gel bond, which has a hydrophobic and a hydrophilic side. Eight- to ten-day-old conidia of strains HyPer9-2 and 4091-5-8 were collected and applied to the hydrophobic surface of gel bond. Images were taken every 15 min during an overnight time course to follow the formation of germ tubes. As shown in Fig. S2b (see Supporting Information), MoHyPer detected higher H_2O_2 levels at 3 h post-inoculation (hpi), indicated by the red–orange colour (blue–purple represents low levels of H_2O_2). As the germ tube forms, MoHyPer detects higher levels of H_2O_2 in the germ tubes, as shown in Movie S1 (see Supporting Information). We examined germination events at different individual time points, and observed H_2O_2 levels in appressoria at 8 hpi (Figs S2c and 4). The MoHyPer protein was also sufficiently sensitive to detect changes in H_2O_2 levels during the germination process. As shown in Fig. S2, an increase in H_2O_2 levels was detected in the three conidial nuclei as the appressorium matured, as indicated by the increases in orange and red colours. As germination progressed through 14 h, we observed that H_2O_2 was detected mostly in the appressorium, with little or no H_2O_2 in the conidium, as shown in Fig. 4, and as expected based on Egan *et al.* (2007).

MoHyPer can detect H_2O_2 changes during the infection process

To investigate whether MoHyPer was able to detect H_2O_2 level changes during plant infection, conidia of MoHyPer 9-2 and wild-type 4091-5-8 strains were applied to the barley leaf surface. Images were taken using confocal microscopy at 21 (Fig. 5), 48 and 72 hpi (Fig. 6). MoHyPer in HyPer 9-2 was able to detect H_2O_2 in infection hyphae as indicated by the red–orange colour in

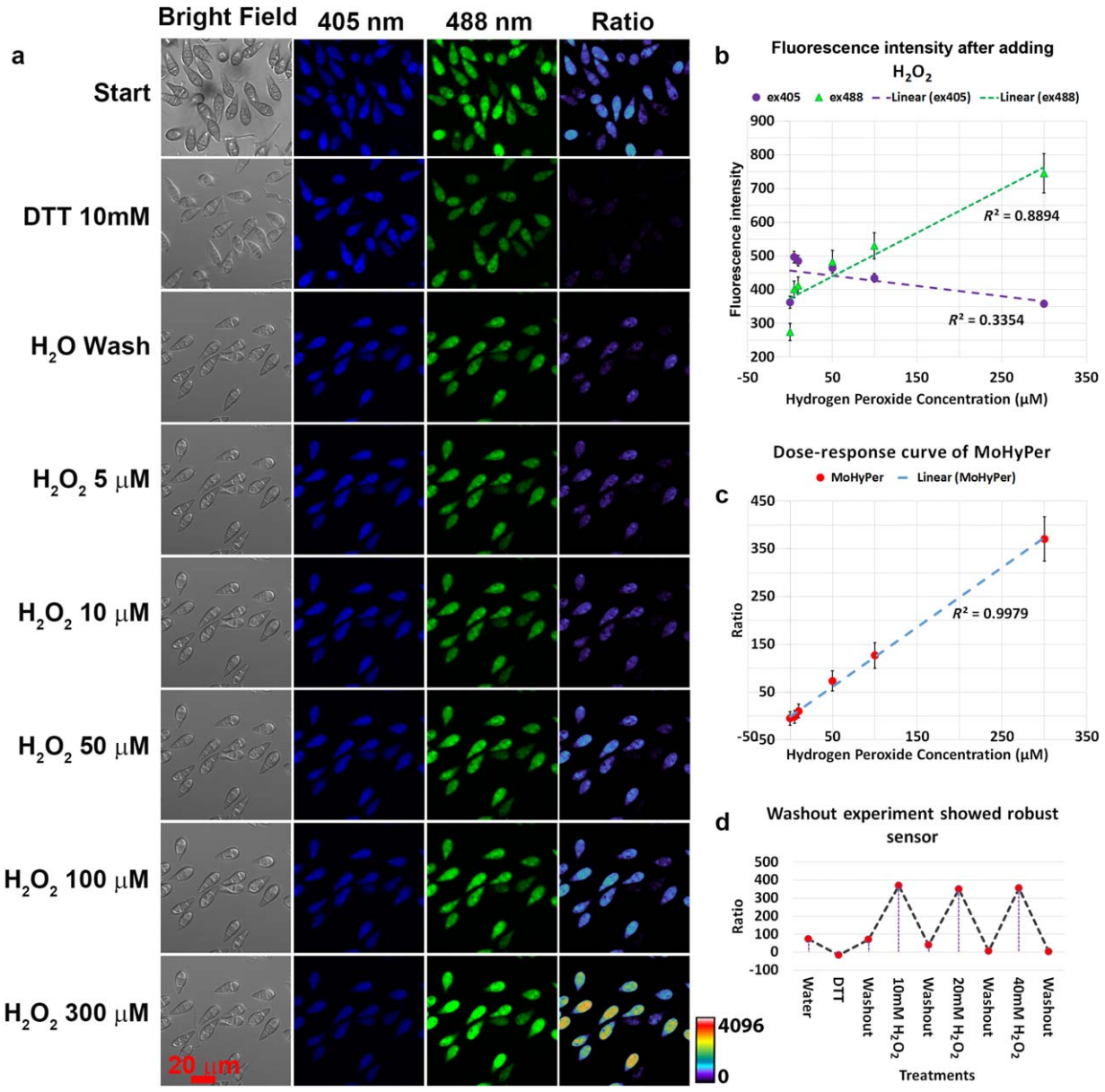

Fig. 3 Response of MoHyPer to exogenous oxidative stress in *Magnaporthe oryzae* conidia. (a) The response to exogenous oxidative stress was measured for conidia at 20 min post-inoculation with increasing concentration of H_2O_2. (b) Dose–response curve of MoHyPer in response to exogenous H_2O_2. (c) MoHyPer was robust and able to detect higher concentrations of H_2O_2. (d) Sterile water washout was carried out between each concentration. All conidia were measured for calculation. DTT, dithiothreitol.

the ratio channel (Fig. 6). Although HyPer 9-2 is a barley-infecting strain, we were able to obtain similar results in young, highly susceptible rice first true leaves through 72 hpi (Fig. S3, see Supporting Information), probably because Maratelli is extremely susceptible in our hands, and detached leaves were inoculated with concentrated droplets of conidia.

Interestingly, we observed higher H_2O_2 levels, as detected by MoHyPer, in newly forming infection hyphae (Fig. S4, see Supporting Information) and a gradual drop in H_2O_2 levels in hyphae from previously colonized cells. We observed little autofluorescence from either the fungus or the plant, and the autofluorescence that was observed was easily distinguishable from the MoHyPer signal. To demonstrate this, we measured emission spectra from the appressoria (MoHyPer sensor), as well as the area around the appressoria (autofluorescence from the plant–pathogen interface), and the two exhibited markedly different spectra, as shown in Fig. S5 and S6 (see Supporting Information).

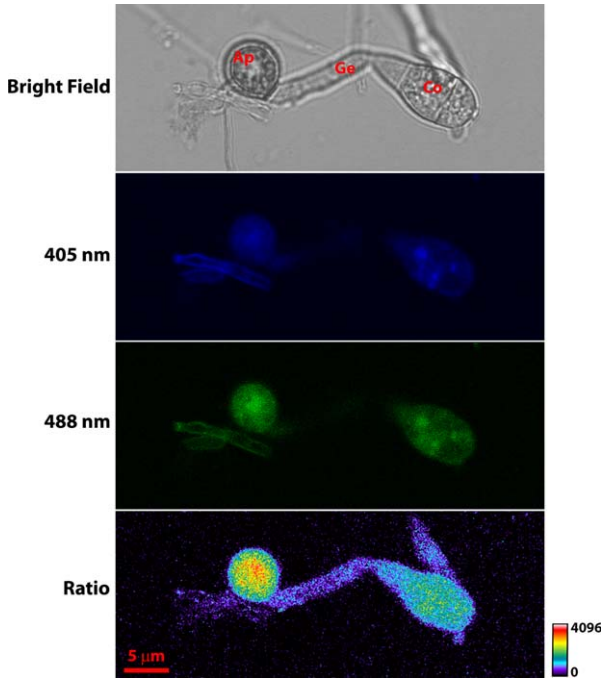

Fig. 4 Detection of H_2O_2 increase in the more mature appressorium. Images were taken at 14 h post-inoculation (hpi) on gel bond. As shown by the scale bar, warmer colours indicate increased levels of H_2O_2. Scale bar, 5 μm. Ap, appressorium; Co, conidium; Gt, germination tube.

MoHyPer can be used to quantify H_2O_2

To further investigate the application of MoHyPer in the detection of H_2O_2 levels during infection, we used two detection methods to quantify H_2O_2 in the HyPer 9-2 strain. As explained previously, the first method employed confocal microscopy using two different excitation wavelengths and determining their ratio. This represented the H_2O_2 level as detected by the MoHyPer sensor. Both the HyPer 9-2 strain and the wild-type 4091-5-8 strain were imaged at the same laser intensity and gain. As shown in Fig. 7a, a higher level of H_2O_2 was observed in the HyPer 9-2 strain. The second method employed a Perkin-Elmer Multilabel Counter 1420 plate reader (Perkin-Elmer Life Sciences, Warwick, RI, USA). In this case, we used 424 and 485 nm for excitation of the blue and green channels. Conidia were collected from oatmeal agar medium (OAM) and applied to 96-well, clear-bottomed plates in water. Figure 7b shows that the H_2O_2 levels are significantly higher in HyPer 9-2 on addition of 3 mM H_2O_2 versus water. The sensor-containing strain showed a higher ratio even without H_2O_2 application, but was still significantly lower than the Hyper 9-2 strain in the presence of H_2O_2.

DISCUSSION

In our study, we have demonstrated the utility of the modified HyPer sensor gene, which we refer to as MoHyPer, to track levels of H_2O_2 during the pre-penetration and penetration events of the rice blast fungus, *M. oryzae*. In order to achieve stable and consistent expression of this gene in the fungus, we had to optimize the codon usage of the original HyPer construct (Belousov *et al.*, 2006) based on the codon usage for the closely related fungus *N. crassa*. The MoHyPer construct ensures stable expression and fluorescence detection of H_2O_2 levels both *in vitro* and *in planta*.

In the *in vitro* condition on gel bond, we observed higher levels of H_2O_2 in asexual spores after the addition of exogenously applied H_2O_2, indicating that the sensor was working as expected, which allowed its use for pre-penetration, initial penetration and infection events. Previously, Samalova *et al.* (2013) used a different type of sensor to study anti-oxidant changes during rice blast infection. Their sensor was a redox-sensitive version of GFP linked to a subunit of GRx, which is a central component of the anti-oxidant GSH. They observed oxidation during appressorial formation, but reduction once it had matured. We made similar observations with the MoHyPer sensor, seeing increased detection of H_2O_2 during appressorial formation around 8 h. In contrast with their results, we continued to observe H_2O_2 in mature appressoria (~21 hpi). These data agree with previous H_2DCFDA-based observations that *M. oryzae* accumulates H_2O_2 during infection-related development (Egan *et al.*, 2007) and around the penetration area.

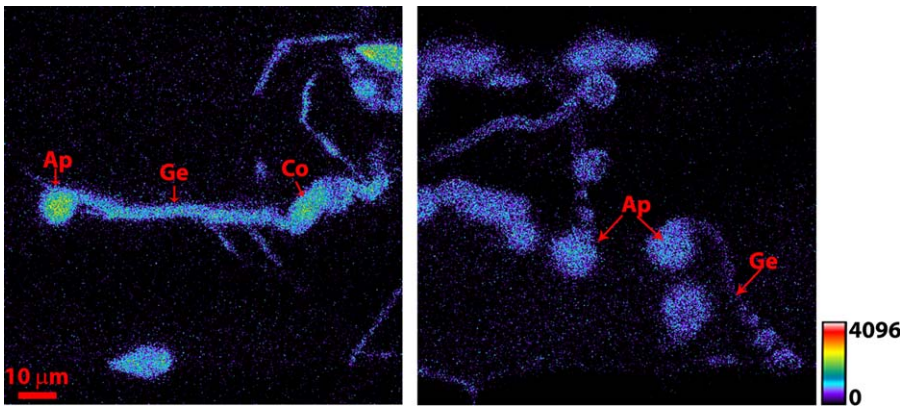

Fig. 5 Appressorium formation on the barley leaf surface at 21 h post-inoculation. (a) *Magnaporthe oryzae* harbouring MoHyPer detected H_2O_2 levels in appressoria. (b) Autofluorescence from wild-type 4091-5-8 conidia. As shown by the scale bar, warmer colours indicate increased levels of H_2O_2. Scale bar = 10 μm for both images. Ap, appressorium; Co, conidium; Gt, germination tube.

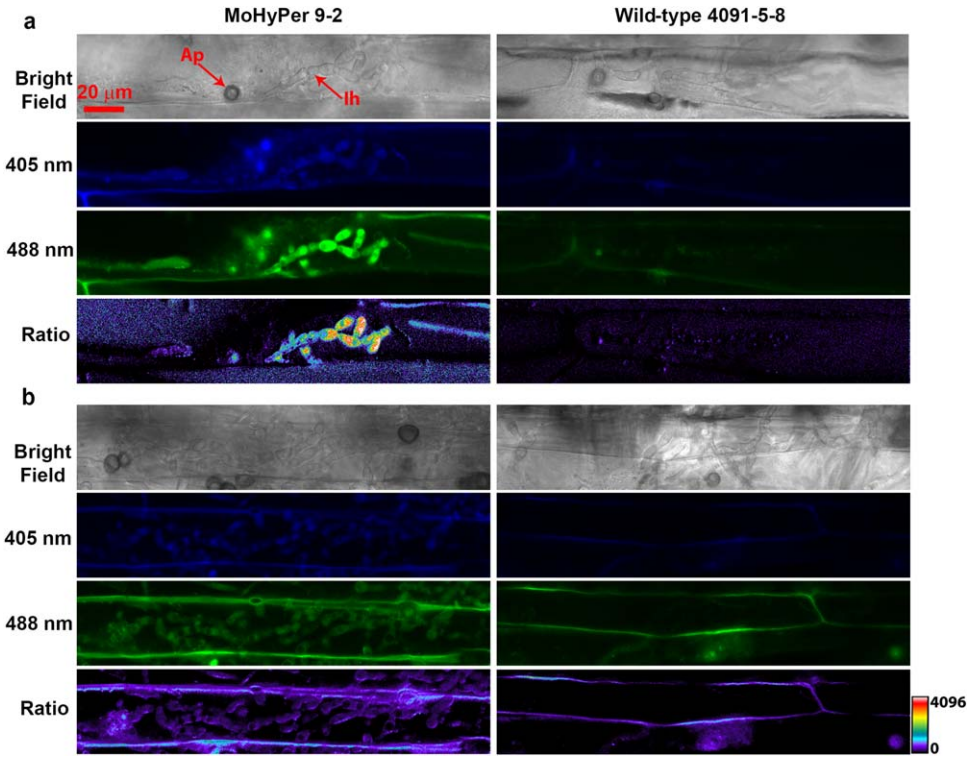

Fig. 6 MoHyPer detected the H_2O_2 level during infection of barley leaf at 48 (a) and 72 h post-inoculation (b). Scale bar = 20 μm for all images. Green channel shows 488-nm wavelength excitation and 516-nm emission. Blue channel shows 405-nm wavelength excitation and 516-nm emission. Ratio channel shows activity of the MoHyPer protein. Ap, appressorium; Ih, infection hyphae.

A continuous challenge with ROS-detecting stains and dyes has been the imaging of plant tissue during later infection stages, beyond the initial infected cell. Previous research has demonstrated the presence of ROS during the interaction at later time points using fluorescent protein fusions with genes involved in, for example, ROS scavenging, such as the *CHAP1* gene in the maize pathogen *Cochliobolus heterostrophus* (Lev *et al.*, 2005). Their research demonstrated that the redox-sensitive CHAP1 transcription factor localized to the nucleus during initial infection events, and remained in the nucleus during later infection stages. Mentges and Bormann (2015) used the HyPer sensor in the plant-pathogenic fungus *Fusarium graminearum* and observed differences between runner hyphae and hyphae that form infection cushions. Their results indicated a higher accumulation of H_2O_2 in infective hyphae compared with the morphologically distinct runner hyphae. Our sensor was able to detect H_2O_2 during the later infection stages of 48 and 72 h, indicating the presence of ROS in the fungal hyphae. Particularly during the 48-h time point, when *M. oryzae* switches from biotrophic, bulbous hyphae to the morphologically distinct invasive, thinner hyphae, we observed increased H_2O_2 detection in newly emerging hyphal tips, and a lack of detection in older hyphae from previously colonized cells.

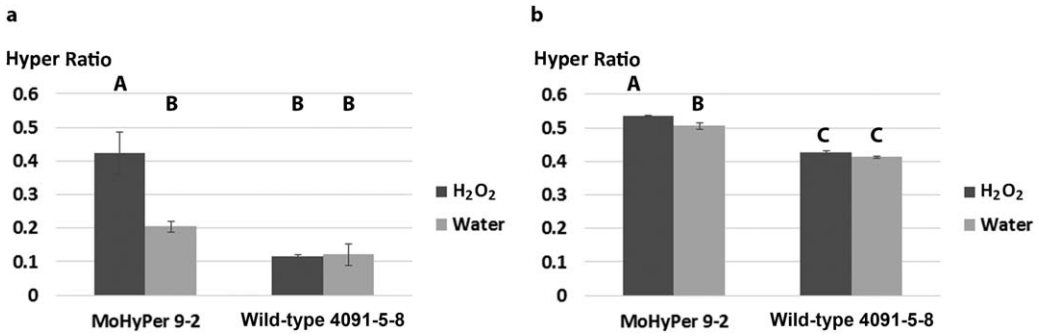

Fig. 7 MoHyPer can be used for H_2O_2 level quantification. Ratios were significantly higher in the HyPer9-2 strain. (a) Values were obtained through confocal images (2 mM H_2O_2 was applied); green and blue channel intensities were divided in order to obtain ratios. (b) Values were obtained directly from the plate reader (3 mM H_2O_2 was applied). Letters indicate significance level at $P < 0.05$. The *y*-axis indicates the ratio taken by dividing the reading from the green channel by that from the blue channel.

This corroborates both the *CHAP1* and *F. graminearum* data, and presents two potential hypotheses: (i) that the fungus is either being challenged by, and processing, or ameliorating the effects of, ROS generated by host basal immune defences; or (ii) as the fungus moves into a more necrotrophic stage, it is generating and secreting ROS as a means of both defence against, and attack of, the host plant. The former hypothesis could be tested by treating the plant with ROS scavengers and performing the same time course with the HyPer 9-2 strain to observe whether H_2O_2 detection is abolished. Additional, more detailed time courses using the sensor will provide insights into the fluctuations in ROS production during all stages of plant infection; when coupled with ROS-defective mutants, such as Δ*hyr1* and Δ*gtr1*, the sensor will prove to be even more valuable in determining how fungal genetic components regulate fluxes in H_2O_2 during infection.

MoHyPer can be used as a robust, dynamic and powerful tool to study ROS generation and dynamics during development and infection of the rice blast fungus. As demonstrated in this study, it can be used to measure changes in H_2O_2 during real time via imaging techniques. In addition, it can be employed to obtain relative quantitative data using a plate reader. The plate reader application makes our sensor extremely easy to use for a range of different studies. One example of how this sensor could be applied would be to use it in conjunction with *M. oryzae* mutants important in redox balance during infective development. Genes involved in the anti-oxidant pathway, including, but not limited to, *HYR1* and *GTR1*, have already been shown to play important roles in the detoxification of plant-produced ROS, hence aiding in pathogen virulence (Fernandez and Wilson, 2014). The *yAP1* gene likewise aids in the detoxification of ROS, but also shows aberrant redox balance during conidiogenesis (Guo *et al.*, 2011). Application of the MoHyPer sensor to this mutant would provide much-needed insight into the role of ROS during conidial formation. The generation of these deletion mutants in the MoHyPer background would help to explain the redox status during pre-penetration and penetration events by imaging how the levels change during development and infection. The plate reader method is easy to apply and is an excellent tool for high-throughput screening. Its optimized codon bias based on *N. crassa* makes it likely that this construct would be applicable to many ascomycete fungi.

EXPERIMENTAL PROCEDURES

M. oryzae strains, growth conditions and plate reader assay

Barley-infecting *M. oryzae*, strain 4091-5-8, was used as the wild-type strain throughout this project, and the strain from which mutants and transgenics were derived. All strains were maintained at 25 °C under constant fluorescent light on complete medium (CM; 1 L: 10 g sucrose, 6 g yeast extract, 6 g casamino acids, 1 mL trace elements). OAM (1 L: 50 g oatmeal and 15 g agar) was used for sporulation. Conidia were harvested 8–10 days after plating. For the plate reader assay, conidia were passed through a sterile miracloth (EMD Millipore, Billerica, MA, USA) filter and suspended in sterile water. Approximately 200 μL of conidial suspension (1×10^5 spores/mL) were pipetted into a 96-well plate, with or without 3 mM H_2O_2, and plates were read in a Perkin-Elmer VICTOR3V 1420 Multilabel Counter plate reader. Experiments were repeated three times.

Plant cultivars and growth conditions

Rice cultivar Maratelli (a gift from the Dean Laboratory, Raleigh, NC, USA) and barley cultivar Lacey (Johnny's Selected Seeds, Winslow, ME, USA) were used throughout this study. Rice was grown in a growth chamber at 80% humidity with a 12 h : 12 h day/night cycle at 28 °C. Barley was grown in a growth chamber at 60% humidity with a 12 h : 12 h day/night cycle at 24 °C (day) and 22 °C (night).

Generation of the MoHyPer construct

We utilized the DuPont Codon Optimizer Site in order to compare codon usage between the HyPer construct (GenBank Submission ID 1871381) and the *M. oryzae* genome. Fourteen pairs of primers were developed that spanned the entire HyPer gene and, at the same time, incorporated appropriate codon bias into the newly synthesized MoHyPer gene (Table S1). Serial PCR was performed using Phusion Hot Start II (ThermoFisher Scientific, Waltham, MA, USA) employing the primer pairs in the order in which they are listed in Table S1 as follows: initial denaturation at 98°C for 30 s; 30 cycles of 98°C for 10 s, 60°C for 15 s and 72°C for 30 s; final extension at 72°C for 5 min; hold at 4°C. The MoHyPer construct sequence was submitted to the National Center for Biotechnology Information (NCBI) and has the current submission number of 1871381.

Cloning of MoHyPer and transformation

An Rp27::MoHyPer construct was generated by fusion PCR. Briefly, using the final product of the serial PCR as a template, MoHyPer with *Bst*EII and *Spe*I sites was amplified with edge primers (Table S1). The resulting 1.4-kb PCR product was generated with *Bst*EII and *Spe*I restriction enzymes (New England Biolabs, Beverly, MA, USA) and cloned into pBlueScript II SK+ (modified by James A. Sweigard, with a Bialaphos-resistant site, named pJS114; it contains the *M. oryzae* RP27 promoter and the *N. crassa* B-tubulin terminator). The construct was fully sequenced and found to be correct; hence, it was transformed into *M. oryzae* strain 4091-5-8 protoplasts to make HyPer transformants (heretofore referred to as HyPer 9-2). Transformants with expected genetic integration events were identified by PCR using the same edge primers (Table S1).

Gel bond and plant inoculation

For gel bond assay, conidia were harvested from 10-day-old cultures grown on OMA in 20 μL of water suspension, for a final concentration of $(1–5) \times 10^5$ conidia/mL. A 50-μL suspension was inoculated on gel bond and kept in a humid chamber overnight. For plant inoculations, 3-week-old leaves of the rice cultivar Maratelli (detached leaves) were prepared according to the protocol of Kankanala *et al.* (2007). In our hands, Maratelli is extremely susceptible to virulent races of *M. oryzae*. For the barley

inoculations, 1-week-old Lacey leaves were detached and laid flat in a humid chamber (90-mm Petri dish with moist filter paper). Twenty microlitres of conidial suspension at the concentration listed above were dropped onto each leaf and the leaves were kept in the dark overnight at approximately 25 °C. The next day, the remaining water droplets were wicked off and the leaves were moved to a growth chamber under constant fluorescent light until imaging at 21, 48 and 72 hpi. Each experiment was repeated at least twice with eight leaves each time.

Treatment with H_2O_2 and washout assay

Eight- to ten-day-old conidia were harvested and inoculated on Ibidi eight-well, non-coated chambers (Ibidi USA, Inc., Madison, WI, USA), 10 min before imaging, and 10 mM DTT (Sigma-Aldrich, St. Louis, MO, USA) was added to reduce background fluorescence. Then, we added sterile water to the well multiple times to wash off non-attached conidia. Afterwards, each concentration of H_2O_2 (Sigma-Aldrich) was applied to the sample and imaged. For the washout assay, after each H_2O_2 treatment, conidia were washed using sterile water twice before adding the next concentration of H_2O_2. Each experiment was repeated three times.

Confocal microscopy and ratiometric analysis

For all the *in vitro* experiments, confocal images were taken with a Zeiss LSM780 (Peabody, MA, USA) using a C-Apochromat 40× (NA = 1.2) water immersion objective lens. MoHyPer was excited at 405 and 488 nm and fluorescence was detected using a 505–550-nm bandpass filter. The ratiometric channel was obtained using the formula:

$$\text{Ratio} = \frac{\text{Channel 1} + 1.00}{\text{Channel 2} + 1.00} \times 1000.00 + (-300.00)$$

(This formula can be changed depending on the different imaging system used.)

Here, the 488/516-nm readout was used as channel 1 and the 405/516-nm readout was used as channel 2. We employed a 3 × 3 median filter for all of our ratio images, with all images being treated equally. We also used transmitted light and reflected light for several confocal experiments, where indicated. For the *in planta* time-course experiments through 72 hpi, the plant inoculation images were taken with a Zeiss LSM880 using a 40× water lens with perfluorodecalin (Sigma-Aldrich) mounting. Each confocal image was taken as a z-stack, followed by maximum projection to obtain the two-dimensional image. Figure S4 and Movie S2 (see Supporting Information) were processed using Amira 3D Software for Life Sciences (FEI, Hillsboro, OR, USA).

ACKNOWLEDGEMENTS

The authors would like to particularly thank Saritha Kunjeti in the Donofrio laboratory for barley and *M. oryzae* growth and maintenance. This project was supported in part by Agriculture and Food Research Initiative Competitive Grant no. 2007-35319-18184 from the USDA National Institute of Food and Agriculture.

AUTHOR CONTRIBUTIONS

NMD, KH, JC and KJC were involved in the conception, design, analysis, interpretation of the data, writing of the manuscript and final approval. JAS was involved in the conception, design and construction of the MoHyPer construct, analysis and editing of the manuscript.

REFERENCES

Belousov, V.V., Fradkov, A.F., Lukyanov, K.A., Staroverov, D.B., Shakhbazov, K.S., Terskikh, A.V. and Lukyanov, S. (2006) Genetically encoded fluorescent indicator for intracellular hydrogen peroxide. *Nat. Methods*, **3**, 281–286.

Bourett, T.M., Sweigard, J.A., Czymmek, K.J., Carroll, A. and Howard, R.J. (2002) Reef coral fluorescent proteins for visualizing fungal pathogens. *Fungal Genet. Biol.* **37**, 211–220.

Brown, S.H., Yarden, O., Gollop, N., Chen, S., Zveibil, A., Belausov, E. and Freeman, S. (2008) Differential protein expression in *Colletotrichum acutatum*: changes associated with reactive oxygen species and nitrogen starvation implicated in pathogenicity on strawberry. *Mol. Plant Pathol.* **9**, 171–190.

Brubacher, J.L. and Bols, N.C. (2001) Chemically de-acetylated 2′,7′-dichlorodihydrofluorescein diacetate as a probe of respiratory burst activity in mononuclear phagocytes. *J. Immunol. Methods*, **251**, 81–91.

Bystrom, L.M., Guzman, M.L. and Rivella, S. (2013) Iron and reactive oxygen species: friends or foes of cancer cells? *Antioxid. Redox Signal*, **20**, 1917–1924.

Choi, H., Kim, S., Mukhopadhyay, P., Cho, S., Woo, J., Storz, G. and Ryu, S.E. (2001) Structural basis of the redox switch in the OxyR transcription factor. *Cell*, **105**, 103–113.

Collinge, D.B. (2009) Cell wall appositions: the first line of defence. *J. Exp. Bot.* **60**, 351–352.

Cruz de Carvalho, M.H. (2008) Drought stress and reactive oxygen species: production, scavenging and signaling. *Plant Signal. Behav.* **3**, 156–165.

Dawe, A.L., McMains, V.C., Panglao, M., Kasahara, S., Chen, B. and Nuss, D.L. (2003) An ordered collection of expressed sequences from *Cryphonectria parasitica* and evidence of genomic microsynteny with *Neurospora crassa* and *Magnaporthe grisea*. *Microbiology*, **149**, 2373–2384.

Dean, R.A., Talbot, N.J., Ebbole, D.J., Farman, M.L., Mitchell, T.K., Orbach, M.J., Thon, M., Kulkarni, R., Xu, J.R., Pan, H., Read, N.D., Lee, Y.H., Carbone, I., Brown, D., Oh, Y.Y., Donofrio, N., Jeong, J.S., Soanes, D.M., Djonovic, S., Kolomiets, E., Rehmeyer, C., Li, W., Harding, M., Kim, S., Lebrun, M.H., Bohnert, H., Coughlan, S., Butler, J., Calvo, S., Ma, L.J., Nicol, R., Purcell, S., Nusbaum, C., Galagan, J.E. and Birren, B.W. (2005) The genome sequence of the rice blast fungus *Magnaporthe grisea*. *Nature*, **434**, 980–986.

Delledonne, M., Zeier, J., Marocco, A. and Lamb, C. (2001) Signal interactions between nitric oxide and reactive oxygen intermediates in the plant hypersensitive disease resistance response. *Proc. Natl. Acad. Sci. USA*, **98**, 13 454–13 459.

Egan, M.J., Wang, Z.Y., Jones, M.A., Smirnoff, N. and Talbot, N.J. (2007) Generation of reactive oxygen species by fungal NADPH oxidases is required for rice blast disease. *Proc. Natl. Acad. Sci. USA*, **104**, 11 772–11 777.

Fernandez, J. and Wilson, R.A. (2014) Characterizing roles for the glutathione reductase, thioredoxin reductase and thioredoxin peroxidase-encoding genes of *Magnaporthe oryzae* during rice blast disease. *PLoS One*, **9**, e87300.

Foreman, J., Demidchik, V., Bothwell, J.H., Mylona, P., Miedema, H., Torres, M.A., Linstead, P., Costa, S., Brownlee, C., Jones, J.D., Davies, J.M. and Dolan, L. (2003) Reactive oxygen species produced by NADPH oxidase regulate plant cell growth. *Nature*, **422**, 442–446.

Guo, M., Chen, Y., Du, Y., Dong, Y., Guo, W., Zhai, S., Zhang, H., Dong, S., Zhang, Z., Wang, Y., Wang, P. and Zheng, X. (2011) The bZIP transcription factor MoAP1 mediates the oxidative stress response and is critical for pathogenicity of the rice blast fungus *Magnaporthe oryzae*. *PLoS Pathog.* **7**, e1001302.

Heller, J. and Tudzynski, P. (2011) Reactive oxygen species in phytopathogenic fungi: signaling, development, and disease. *Annu. Rev. Phytopathol.* **49**, 369–390.

Heller, J., Meyer, A.J. and Tudzynski, P. (2012) Redox-sensitive GFP2: use of the genetically encoded biosensor of the redox status in the filamentous fungus *Botrytis cinerea*. *Mol. Plant Pathol.* **13**, 935–947.

Huang, K., Czymmek, K.J., Caplan, J.L., Sweigard, J.A. and Donofrio, N.M. (2011) HYR1-mediated detoxification of reactive oxygen species is required for full virulence in the rice blast fungus. *PLoS Pathog.* **7**, e1001335.

Kankanala, P., Czymmek, K. and Valent, B. (2007) Roles for rice membrane dynamics and plasmodesmata during biotrophic invasion by the blast fungus. *Plant Cell*, **19**, 706–724.

Kawano, T. (2003) Roles of the reactive oxygen species-generating peroxidase reactions in plant defense and growth induction. *Plant Cell Rep.* **21**, 829–837.

Lang, P.A., Xu, H.C., Grusdat, M., McIlwain, D.R., Pandyra, A.A., Harris, I.S., Shaabani, N., Honke, N., Maney, S.K., Lang, E., Pozdeev, V.I., Recher, M., Odermatt, B., Brenner, D., Häussinger, D., Ohashi, P.S., Hengartner, H., Zinkernagel, R.M., Mak, T.W. and Lang, K.S. (2013) Reactive oxygen species delay control of lymphocytic choriomeningitis virus. *Cell Death Differ.* **20**, 649–658.

Lev, S., Hadar, R., Amedeo, P., Baker, S.E., Yoder, O.C. and Horwitz, B.A. (2005) Activation of an AP1-like transcription factor of the maize pathogen *Cochliobolus heterostrophus* in response to oxidative stress and plant signals. *Eukaryot. Cell*, **4**, 443–454.

Mentges, M. and Bormann, J. (2015) Real-time imaging of hydrogen peroxide dynamics in vegetative and pathogenic hyphae of *Fusarium graminearum*. *Sci. Rep. UK*, **5**, 14980.

Mittler, R., Vanderauwera, S., Gollery, M. and Van Breusegem, F. (2004) Reactive oxygen gene network of plants. *Trends Plant Sci.* **9**, 490–498.

Panieri, E., Gogvadze, V., Norberg, E., Venkatesh, R., Orrenius, S. and Zhivotovsky, B. (2013) Reactive oxygen species generated in different compartments induce cell death, survival, or senescence. *Free Radic. Biol. Med.* **57**, 176–187.

Parker, D., Beckmann, M., Enot, D.P., Overy, D.P., Rios, Z.C., Gilbert, M., Talbot, N. and Draper, J. (2008) Rice blast infection of *Brachypodium distachyon* as a model system to study dynamic host/pathogen interactions. *Nat. Protoc.* **3**, 435–445.

Rogers, S.A. (2002) *Detoxify or Die*. Sarasota, FL: Sand Key Company.

Ronen, M., Shalaby, S. and Horwitz, B.A. (2013) Role of the transcription factor ChAP1 in cytoplasmic redox homeostasis: imaging with a genetically encoded sensor in the maize pathogen *Cochliobolus heterostrophus*. *Mol. Plant Pathol.* **14**, 786–790.

Samalova, M., Meyer, A.J., Gurr, S.J. and Fricker, M.D. (2013) Robust antioxidant defences in the rice blast fungus *Magnaporthe oryzae* confer tolerance to the host oxidative burst. *New Phytol.* **201**, 556–573.

Schurmann, J., Buttermann, D., Herrmann, A., Giesbert, S. and Tudzynski, P. (2013) Molecular characterization of the NADPH oxidase complex in the ergot fungus *Claviceps purpurea*: CpNox2 and CpPls1 are important for a balanced host–pathogen interaction. *Mol. Plant–Microbe Interact.* **26**, 1151–1164.

Skamnioti, P., Henderson, C., Zhang, Z., Robinson, Z. and Gurr, S.J. (2007) A novel role for catalase B in the maintenance of fungal cell-wall integrity during host invasion in the rice blast fungus *Magnaporthe grisea*. *Mol. Plant–Microbe Interact.* **20**, 568–580.

Sun, S., Wang, H., Yu, H., Zhong, C., Zhang, X., Peng, J. and Wang, X. (2013) GASA14 regulates leaf expansion and abiotic stress resistance by modulating reactive oxygen species accumulation. *J. Exp. Bot.* **64**, 1637–1647.

Tarpey, M.M., Wink, D.A. and Grisham, M.B. (2004) Methods for detection of reactive metabolites of oxygen and nitrogen: in vitro and in vivo considerations. *Am. J. Physiol. Regul. Integr. Comp. Physiol.* **286**, R431–R444.

ThordalChristensen, H., Zhang, Z.G., Wei, Y.D. and Collinge, D.B. (1997) Subcellular localization of H_2O_2 in plants. H_2O_2 accumulation in papillae and hypersensitive response during the barley–powdery mildew interaction. *Plant J.* **11**, 1187–1194.

Valent, B., Farrall, L. and Chumley, F.G. (1991) *Magnaporthe-grisea* genes for pathogenicity and virulence identified through a series of backcrosses. *Genetics*, **127**, 87–101.

Wilson, R.A. and Talbot, N.J. (2009) Under pressure: investigating the biology of plant infection by *Magnaporthe oryzae*. *Nat. Rev. Microbiol.* **7**, 185–195.

Yang, S.L. and Chung, K.R. (2012) The NADPH oxidase-mediated production of hydrogen peroxide (H_2O_2) and resistance to oxidative stress in the necrotrophic pathogen *Alternaria alternata* of citrus. *Mol. Plant Pathol.* **13**, 900–914.

Yang, S.L., Lin, C.H. and Chung, K.R. (2009) Coordinate control of oxidative stress tolerance, vegetative growth, and fungal pathogenicity via the AP1 pathway in the rough lemon pathotype of *Alternaria alternata*. *Physiol. Mol. Plant Pathol.* **74**, 100–110.

SUPPORTING INFORMATION

Additional Supporting Information may be found in the online version of this article at the publisher's website:

Table S1 Primers for MoHyPer synthesis.

Table S2 Codon usage frequency for *Magnaporthe oryzae* and HyPer.

Fig. S1 Polymerase chain reaction (PCR) confirmation of transformed *Magnaporthe oryzae*. Primers flanking the entire length of Hyper-AS sensor proteins were used against total DNA from transformed Magnaporthe 9-2 (lane 2), 4091-5-8 control (lane 3) and positive vector control that has a Hyper-AS sequence (lane 4). Lane 5 is a no template control. Lanes 1 and 6 are 1- kb and 100-bp DNA ladders from New England Biolabs, Beverly, MA, USA. The bottom panel shows a diagram of the construct used for transformation.

Fig. S2 Time course of appressorium formation on gel bond in the MoHyPer9-2 strain. As detected by the MoHyPer sensor, H_2O_2 appears to increase during appressorial formation. As shown by the scale bar, warmer colours indicate increased levels of H_2O_2. (a) 0 h post-inoculation (hpi); (b) 3 hpi; (c) 8 hpi; (d) 10 hpi; (e) 11 hpi; (f) 12.5 hpi. Scale bar = 20 μm for all images. Co, conidia; Gt, germination tube.

Fig. S3 MoHyPer detects the H_2O_2 level during infection of rice leaf at 72 h post-inoculation. Scale bar = 20 μm for all images.

Fig. S4 Three-dimensional image of MoHyPer-detected H_2O_2 level during infection of barley leaf. MoHyPer detects higher levels of H_2O_2 in the newly forming hypha, indicated by the red arrow. Scale bar = 20 μm for all images. Co, conidium.

Fig. S5 Spectra of MoHyPer and plant autofluorescence. MoHyPer shows a spectral peak around 516 nm and autofluorescence is broad and non-specific. Excitation wavelength, 488 nm.

Fig. S6 Series of Movie S1. Scale bar = 5 μm for all images.

Movie S1 MoHyPer sensor detects an increase in H_2O_2 level during the germination process. The movie shows overnight observation of conidial germination on the hydrophobic surface, gel bond.

Movie S2 Three-dimensional rendering of MoHyPer-detected H_2O_2 level during the infection of barley leaf at 48 h post-inoculation.